All-Trans Retinoic Acid Induces XAF1 Expression Through an Interferon Regulatory Factor-1 Element in Colon Cancer

JIDE WANG,*,† YING PENG,§ YUN WEI SUN,† HUA HE,† SENLIN ZHU,† XIAOMENG AN,§ MING LI,§ MARIE C. M. LIN,§ BING ZOU,† HARRY HUA–XIANG XIA,† BO JIANG,* ANNIE O. O. CHAN,† MAN FUNG YUEN,† HSIANG FU KUNG,§ and BENJAMIN C. Y. WONG†

*Institute for Digestive Medicine, Nanfang Hospital, Southern Medical University, Guangzhou, People's Republic of China; and †Department of Medicine, and §Institute of Molecular Biology, University of Hong Kong, Hong Kong, China

Background & Aims: **X-linked inhibitor of apoptosis protein (XIAP)-associated factor 1 (XAF1) is a novel tumor suppressor and interferon (IFN)-stimulated gene. All-trans retinoic acid (ATRA) exerts an antiproliferative effect on tumor cells through up-regulation of IFN regulatory factor 1 (IRF-1) and the downstream IFN-stimulated genes. The aim of this study was to determine the effect and mechanism of ATRA on XAF1 expression and the role of XAF1 in ATRA-induced growth inhibition in colon cancer.** ***Methods:*** **Gene expression is detected by reverse-transcription polymerase chain reaction and immunoblotting. The transcription activity of XAF1 promoter is examined by luciferase reporter assay. The activity of IFN regulatory factor binding element (IRF-E) is assessed by electrophoretic mobility shift assay and chromatin immunoprecipitation assay. Cell growth is evaluated by both in vitro and in vivo in nude mice xenografts.** ***Results:*** **IFN-alfa stimulates XAF1 promoter activity in the colon cancer cells Lovo and SW1116 dose-dependently. An IRF-1 binding element (IRF-E–XAF1) is found in the -30 to -38 nucleotide region upstream of the ATG initiator codon of the XAF1 gene. Site-directed mutagenesis of IRF-E–XAF1 abrogates native and IFN-induced promoter activity and binding capacity. ATRA induces XAF1 expression both in vitro and in vivo through interaction with IRF-E–XAF1. Overexpression of XAF1 increases cell susceptibility to ATRA-induced growth suppression both in vitro and in vivo. Furthermore, the effect of ATRA on XAF1 expression is independent of the promoter methylation and the subcellular distribution of XIAP.** ***Conclusions:*** **XAF1 participates in ATRA-induced growth suppression through IRF-1–mediated transcriptional regulation.**

Inhibitor of apoptosis protein (IAP) is a protein family acting through the inhibition of caspase activity.[1] X-linked IAP (XIAP) is a member of IAP that is expressed in all adult and fetal tissues with the exception of peripheral blood leukocytes.[2] XIAP binds directly to caspases via 1 or more of its baculoviral inhibitory repeat domains and may function as a competitive inhibitor of caspase catalytic function.[2,3] Overexpression of XIAP in cancer cells induces resistance to apoptotic stimuli.[3] Suppression of XIAP by short-interfering RNA (siRNA) or antisense strategy sensitizes cancer cells to apoptosis.[4,5]

XIAP-associated factor 1 (XAF1) is a novel XIAP-interacting protein. It functions as an antagonist of XIAP by rescuing XIAP-suppressed caspase activity.[6,7] The incubation of recombinant XIAP with caspase-3 in the absence or presence of XAF1 showed that XAF1 blocked the inhibitory activity of XIAP for caspase-3, and co-expression of XAF1 and XIAP induced nuclear translocation of XIAP and inhibited XIAP-dependent caspase-3 suppression. XAF1 was implicated as a tumor suppressor based on the observation that expression was lower in tumor including gastric and colon cancer cell lines compared with normal tissues and that transient expression of XAF1 sensitized tumor cells to the pro-apoptotic effects of etoposide.[6–9]

Leaman et al[10,11] have defined XAF1 as a novel IFN-stimulated gene (ISG) associated with interferon-β (IFN-β)–induced apoptosis in melanoma cells. XAF1 messenger RNA (mRNA) was up-regulated by IFN-alfa and IFN-β in all cells examined. Retinoic acid (RA) exerts different effects such as inhibition of proliferation, induction of differentiation, and immunomodulation.[12–15] Both RA and IFNs exert antiproliferative effects on various cell types. Several groups have reported a higher inhibition of cell proliferation by a combination of RA

Abbreviations used in this paper: ATRA, all-trans retinoic acid; EMSA, electrophoretic mobility shift assay; IAP, inhibitor of apoptosis protein; IFN, interferon; IRF-1, interferon regulatory factor 1; IRF-E, interferon regulatory factor binding element; ISG, interferon-stimulated gene; MTT, 3-(4,5-dimethylthiazol-2-yl)-2,5-diphenyltetrazolium bromide; PCR, polymerase chain reaction; RA, retinoic acid; RLU, relative luciferase unit; siRNA, short-interfering RNA; XAF1, X-linked inhibitor of apoptosis protein–associated factor 1; XIAP, X-linked inhibitor of apoptosis protein.

0016-5085/06/$32.00
doi:10.1053/j.gastro.2005.12.017

with IFN, compared with treatment by each agent alone.[15,16] However, the mechanism of this collaborative effect has not been elucidated fully. It has been shown recently that RA up-regulates interferon regulatory factor 1 (IRF-1) gene expression in various cell lines.[17–19]

In this study, we identified a high-affinity IRF-1 binding element (IRF-E) in the promoter of the XAF1 gene. This element mediated the up-regulation of XAF1 expression induced by both IFN and all-trans retinoic acid (ATRA). Consequently, we defined XAF1 as a mediator of ATRA in suppressing colon cancer cell growth.

Materials and Methods

Reagents and Cell Culture

ATRA was purchased from Sigma (St. Louis, MO). IFN-alfa was purchased from Schering-Plough Company (Innishannon, Ireland). Goat anti-human XAF1 (C-16), goat anti-human actin (I-19), rabbit anti-human IRF-1 (C-20), normal rabbit immunoglobulin (Ig)G, horseradish-peroxidase–conjugated anti-goat IgG, and anti-mouse IgG were purchased from Santa Cruz Biotechnology (Santa Cruz, CA). Rabbit anti-human XIAP was purchased from Cell Signal Technology (Beverly, MA). The colon cancer cell lines Lovo and SW1116 were obtained from American Type Culture Collection (Rockville, MD) and maintained in RPMI 1640 medium supplemented with 10% fetal bovine serum, 100 μg/mL streptomycin, and 100 u/mL penicillin in a humidified incubator at 37°C with an atmosphere of 5% CO_2.

Reverse-Transcription Polymerase Chain Reaction

RNA was reverse-transcribed to complementary DNA (cDNA) by Thermoscript reverse-transcription polymerase chain reaction (PCR) system (Invitrogen Life Technologies, Carlsbad, CA) in accordance with the manufacturer's instructions. PCR was performed using 2 μL of resulting cDNA, .3 units of Hotstart DNA polymerase (Qiagen, Hilden, Germany), forward and reverse primers, and deoxynucleoside triphosphates in a final volume of 50 μL. The sequences of the primers were as follows: XAF1 forward: 5′-GCTCCACGAGTCCTACTG-3′; XAF1 reverse: 5′-ACTCTGAGTCTGGACAAC-3′. Hotstart PCR was performed for 33 cycles with 95°C denaturation for 30 minutes (first cycle), 94°C denaturation for 45 seconds, 55°C annealing for 45 seconds, and 72°C elongation for 45 seconds and 10 minutes (final cycle). The amplification product was of the expected sizes (262 bp).

Immunoblotting

Cell lysates (20 μg) were electrophoresed on denaturing sodium dodecyl sulfate–polyacrylamide gel electrophoresis gel (5% stacking gel and 12% separating gel). Proteins were transferred to polyvinylidene difluoride membranes (PerkinElmer, Fremont, CA). Nonspecific binding was blocked with 10 mmol/L pH 7.6 Tris–HCl buffer saline plus .05% Tween-20 containing 2% skim milk. The blots were probed with primary anti-human XAF1 antibody (C-16) followed by the horseradish-peroxidase–conjugated anti-goat second antibody. Antigen-antibody complexes were visualized by the enhanced chemiluminescence (ECL) system (Amersham Biosciences, Little Chalfont, Buckinghamshire, England, UK).

Transient Transfection and Establishment of Lovo Stable Transfectants Expressing XAF-S and XAF-AS

Gene transfection and establishment of stably expressing cell lines were performed as we previously reported.[20,21] For transient transfection, pcDNA3 construct encoding sense or antisense human XAF1 gene (pcDNA3–XAF1-S and pcDNA3–XAF1-AS), pDs-red2-c1-XAF1 expressing XAF1-red fluorescent protein (RFP) fusion protein, or pEGFP-C1-XIAP expressing XIAP-GFP fusion protein (kindly provided by Dr. Korneluk)[7] were mixed with serum medium containing LipofectAMINE2000 reagent (Invitrogen). RFP- or GFP-fused proteins were observed under a Zeiss Axioscop fluorescence microscope (Oberkochen, Germany). Nuclei were stained with 1 μg/mL Hoechst 22358. To establish the stable cell lines, Lovo cells transfected with empty pcDNA3 vector, pcDNA3–XAF1-S, or pcDNA3–XAF1-AS as mentioned previously were passaged at 1:15 (vol/vol) and cultured in medium supplemented with Geneticin (G418, Sigma) at 1000 μg/mL for 4 weeks. Stably transfected clones were selected by immunoblotting for XAF1 expression and maintained in medium containing 600 μg/mL G418 for additional studies.

Generation of XAF1 Promoter-Luciferase Constructs

We have identified the transcription starting site of the XAF1 gene located at –26 nt upstream of the ATG translation initiator codon (unpublished data) by the rapid amplification of 5′-cDNA ends (5′-RACE) assay. We cloned a regulatory segment of the 5′-flanking region of the XAF1 gene containing the core promoter region. pLUC107 contained –107∼164 nt segment of the XAF1 gene. The upstream nucleotide adjacent to the translation initiator ATG codon was defined here as –1. The primers were as follows: pLUC107 forward: 5′-GATCTCCTCCCTCCCTGAA-3′, reverse: 5′-GTCTCCAGCTGCTTGTCCTC-3′. The Kpn I site was added into the 5′ terminus of the forward primers and the XhoI site was added into the reverse primer. Genomic DNA of a Lovo cell was used as the template for PCR amplification with Hotstart *Taq* polymerase. PCR products were visualized on 1% agarose gels by ethidium bromide staining and purified using GFX PCR DNA and the Gel Band Purification Kit (Amersham Biosciences). After digestion of both the pGL3basic vector (Promega, Madison, WI) and the PCR products with Kpn I and XhoI, the purified products were inserted in the forward orientation upstream of a luciferase reporter gene of the pGL3basic vector to generate promoter/luciferase constructs (pLUC107).

Luciferase Reporter Assay

For luciferase assay, the cells were transfected transiently with pLUC107 by LipofectAMINE2000 as we previously reported.[22] Serum- and antibiotic-free medium containing XAF1 promoter reporter plasmids and pRL-CMV vector was mixed with LipofectAMINE2000 reagent and various cell lines. Forty-eight hours later, the cells were mixed with 50 μL of luciferase assay reagent (Promega). The firefly and renilla luciferase activities were measured using the Dual-Luciferase reporter system (Promega) with a model TD-20/20 Luminometer (EG&G, Berthold, Australia). The firefly luciferase activity value was normalized to the renilla activity value. Promoter transcription activity was presented as the fold induction of relative luciferase unit (RLU) compared with basic pGL3 vector control. (The RLU was the value of the firefly luciferase unit divided by the value of the renilla luciferase unit.)

Electrophoretic Mobility Shift Assay

Double-strand XAF1 gene–specific DNA probe that contained the putative IRF-E sequence was 5′- GCCTGCAAGAAACGAAACTCAACCGA-3′. The IRF-1 consensus probe sequence was: 5′-GGAAGCGAAAATGAAATTGACT-3′. After annealing, double-strand DNA probes were labeled with 5 mCi of γ-^{32}P-ATP (PerkinElmer Life and Analytical Sciences) using T4 polynucleotide kinase (Promega). For electrophoretic mobility shift assay (EMSA), total reaction mixtures containing 10 mmol/L Tris/HCl (pH 7.5), 1 mmol/L $MgCl_2$, .5 mmol/L dithiothreitol, .5 mmol/L ethylenediaminetetraacetic acid, 50 mmol/L NaCl, 4% glycerol, and 50 μg of poly(dI-dC)-poly(dI-C)/mL, were incubated with 3 μg of nuclear extracts and various unlabeled competing oligonucleotides for 10 minutes at room temperature, followed by addition of 1 μL ([.5∼2] × 10^5 counts per minute) of the various ^{32}P–end-labeled oligonucleotides. Samples were separated by electrophoresis on 8% nondenaturing polyacrylamide gel, with detection of radioactive bands by autoradiography for 16–24 hours at −80°C.

siRNA Transfection

The siRNA duplexes consisted of 23 bp with a 2-base deoxynucleotide overhang (Proligo, Singapore). The sequences of the FHL2 siRNA were as follows (sense strand): siRNA 1, GGAAGCGAAAAUGAAAUUGACdTdT. The control siRNA, GL2 (CGUACGCGGAAUACUUCGA) was directed against the luciferase gene. The cells were transfected with siRNA duplexes using Oligofectamine (Invitrogen) according to the manufacturer's instructions.

Chromatin Immunoprecipitation Assay

The chromatin-immunoprecipitation assays were performed according to the protocol provided by the chromatin-immunoprecipitation assay kit (Upstate Cell Signaling Solutions, Lake Placid, NY). Briefly, cells were treated with 1% formaldehyde to cross-link proteins to DNA. After washing, the cell pellets were resuspended in lysis buffer and sonicated to yield an average DNA size of 500 bp. Sonicated extracts subsequently were clarified by centrifugation and diluted with chromatin immunoprecipitation dilution buffer. Twenty microliters of the diluted lysates was left as the input control. Other lysates were precleared with protein A agarose/salmon-sperm DNA and then divided into 2 fractions and incubated with 5 μg of normal rabbit IgG or rabbit anti-human IRF-1 antibody each. Protein A agarose/salmon-sperm DNA was added to each fraction and rotated at 4°C. After thoroughly washing, immunoprecipitated products were eluted using elution buffer. The cross-linked DNA–protein complexes were reversed by heating at 65°C. DNA was purified by phenol/chloroform extraction and ethanol precipitation. Quantitation of the DNA from the XAF1 promoter regions was determined by PCR using gene-specific primers as described later. Hot-start PCR amplification was performed using either immunoprecipitated DNA, a control with rabbit IgG, or chromatin input that had not been immunoprecipitated. To ensure linear amplification of DNA, pilot PCR reactions were performed initially to determine the optimal PCR conditions. In general, samples were heated at 95°C for 30 minutes, followed by 34 cycles of 95°C for 1 minute, 55°C for 1 minute, and 72°C for 1 minute. After cycling, samples were incubated at 72°C for 7 minutes to permit completion of primer extension. The primers used were as follows: sense (–122 to –141) 5′-ATCAAGGGGAACTCCTGAGC-3′ and antisense (+11 to +30): 5′-GTTCCTGCACACCGAGAAGT-3′.

Site-Directed Mutagenesis Analysis

The QuikChange Site-Directed Mutagenesis Kit (Stratagene, La Jolla, CA) was used to generate constructs with the mutation of the putative interferon regulatory element (IRF-E–XAF1, –30 to –38 nt). The primers of mutation were as follows: wild-type sequence: GCCTGCAAGAAACGAAACTCAACCGAAAGCC, –34 mutation: GCCTGCAAGAAAAGAAACTCAACCGAAAGCC, –28 mutation: GCAAGAAACGAAACCCAACCGAAAGCCTGC. Briefly, pLuc-107 construct was PCR-amplified in the elongation process using Pfu DNA polymerase with the earlier-described double-strand primers. The incorporation of oligonucleotide primers generates a mutated plasmid containing staggered nicks. The product then is treated with *Dpn*I endonuclease, specific for methylated and hemimethylated DNA, enabling the parental DNA template to be digested (because DNA originating from *Escherichia coli* usually is *dam* methylated). The nicked vector DNA carrying the desired mutations was proliferated in Epicurian coli XL1-Blue supercompetent cells. Plasmid DNA was isolated and sequenced using the ABI PRISM 377 DNA Sequencer (Applied Biosystems, Inc., Foster City, CA), according to the manufacturer's instructions, to verify the prospected mutated sequence.

Analysis of Gene Methylation: Bisulfite DNA Sequencing

DNA (≃100 ng) was denatured with NaOH and treated with sodium bisulfite for 16 hours (Sigma). Before

sequencing, all cytosine residues were deaminated and converted to thymine residues by sodium bisulfite modification. 5-methylcytosine residues were not altered by this treatment. Fifty nanograms of bisulfite-modified DNA were subjected to PCR amplification of the XAF1 promoter region using primer sets: Bf (sense, 5′-GTTTTGTTTTTT-TGTTTGTAAGAAACG-3′) and Br (antisense, 5′-ATTTA-AACCCTCCTACCCTTAAAAC-3′) for nucleotides from −59 nt to +194 nt (253 bp). The PCR products were cloned into pGEM-T vectors (Promega) and 10 clones of each specimen were sequenced using an ABI PRISM 377 sequencer to determine the methylation status.

3-(4,5-Dimethylthiazol-2-yl)-2,5-Diphenyltetrazolium Bromide Assay

Cytotoxicity was measured by 3-(4,5-dimethylthiazol-2-yl)-2,5-diphenyltetrazolium bromide (MTT) assay. Cells growing exponentially were plated onto 96-well plates at a density of 10,000 cells/well for 18 hours. The cells then were transfected with expressing construct and treated with ATRA for 48 hours. Fifty microliters of MTT stock solution (1 mg/mL) was added to each well and the cells were incubated further at 37°C for 4 hours. The supernatant was replaced with dimethyl sulfoxide to dissolve formazan production. The absorbance at wavelength 570 nm was measured with a micro–enzyme-linked immunosorbent assay reader (Bio-Rad, Hercules, CA). The ratio of the absorbance of treated cells relative to that of the control cells was calculated and expressed as a percentage of cell-growth suppression.

Tumorigenicity in Nude Mice

A nude mice xenograft experiment was performed as we previously reported.[21] Single-cell suspensions of stable Lovo/vector and Lovo/XAF1-S transfectants were trypsinized and collected. Cell viability was greater than 95% as determined by trypan blue exclusive staining. Cells (5×10^6) in a .1-mL volume of RPMI 1640 were inoculated subcutaneously into the right flank of 5- to 6-week-old female BALB/c-*nu*/*nu* mice (Laboratory Animal Unit, The University of Hong Kong). Institution guidelines were followed in handling the animals. After the tumors became palpable, 15 mg/kg of ATRA or dissolvent control (corn oil, .3 mL) were given intraperitoneally once daily for 5 days. Doses and treatment schedules were chosen based on preliminary experiments assessing tolerability and on previously published data.[23,24] Mice were kept for an additional 6 weeks to assess tumor size. The volumes of tumor were calculated as follows: $V = (4/3)\ R1^2\ R2$, where $R1$ is radius 1 and $R2$ is radius 2 and $R1 < R2$. The Committee on the Use of Live Animals in Teaching and Research at the University of Hong Kong approved the protocol.

Statistical Analysis

Results obtained from triplicate luciferase and MTT experiments were expressed as the mean ± SD. RLU with different treatments were compared using a 2-tailed Student *t* test and were considered significant if *P* values were less than .05.

Results

Identification of XAF1 as an ISG

Leaman et al[10,11] classified XAF1 as an ISG. To confirm their findings, we treated colon cancer cells, Lovo, and SW1116 with IFN-alfa. We showed that XAF1 expression was up-regulated at both mRNA and protein levels (Figure 1*A*, *B*). The effect of IFN-alfa was dose dependent at the mRNA level (Figure 1*A*).

We have identified the transcription starting site at −26 nt of the XAF1 gene (data not shown). Thus, we cloned −107 to −164 nt segment that contained the transcription starting site of XAF1 into luciferase reporter plasmid and named it *pLUC107*. Lovo and SW1116 cells transfected with this construct were treated with or without IFN-alfa. As shown in Figure 1*C*, the fold induction of RLU of pLUC107 in Lovo and SW1116 cells were 7.6 and 14, respectively. IFN-alfa increased pLUC107 activities to 61.7% and 87.1% (12.3 ± 1.2 vs 7.6 ± .3 and 26.4 ± 1.2 vs 14 ± .2, in Lovo and SW1116 cells, respectively) ($P <$ .05 compared with untreated control). To clarify the dose effect, SW1116 cells transfected with pLUC107 were treated with 0, 62.5, 125, and 250 units of IFN-alfa. The fold inductions of RLU were 12.1 ± 1.2, 16.2 ± 2.1, 26.8 ± .7, and 48.3 ± 6.6, respectively, suggesting that IFN-alfa up-regulated XAF1 promoter activity in a dose-dependent manner (Figure 1*D*).

Identification of a High-Affinity IRF-E in the Transcription Starting Site of XAF1

By searching the 5′-flanking sequence of XAF1 gene with TFsearch software (http://molsun1.cbrc.aist.go.jp/research/db/TFSEARCH.html), we identified a putative IRF-E with 76.2% of identity to the consensus sequence at the −30 to −38 nt region of the XAF1 gene (Figure 2*A*, underlined sequence).[25]. This sequence was defined as IRF-E–XAF1. To confirm its binding capacity, we first extracted nuclear protein of SW1116 cells with or without IFN-alfa (62.5 u/mL for 12 h). An EMSA assay was performed to check their binding with ^{32}P-labeled double-strand probe of IRF-E–XAF1. As shown in Figure 2*B*, a specific binding band was observed. Furthermore, increasing the concentration of IFN-alfa increased the binding activity slightly (Figure 2*C*). To verify the specificity of binding, we incubated excessive amounts of unlabeled IRF-1 consensus probe before the incubation of nu-

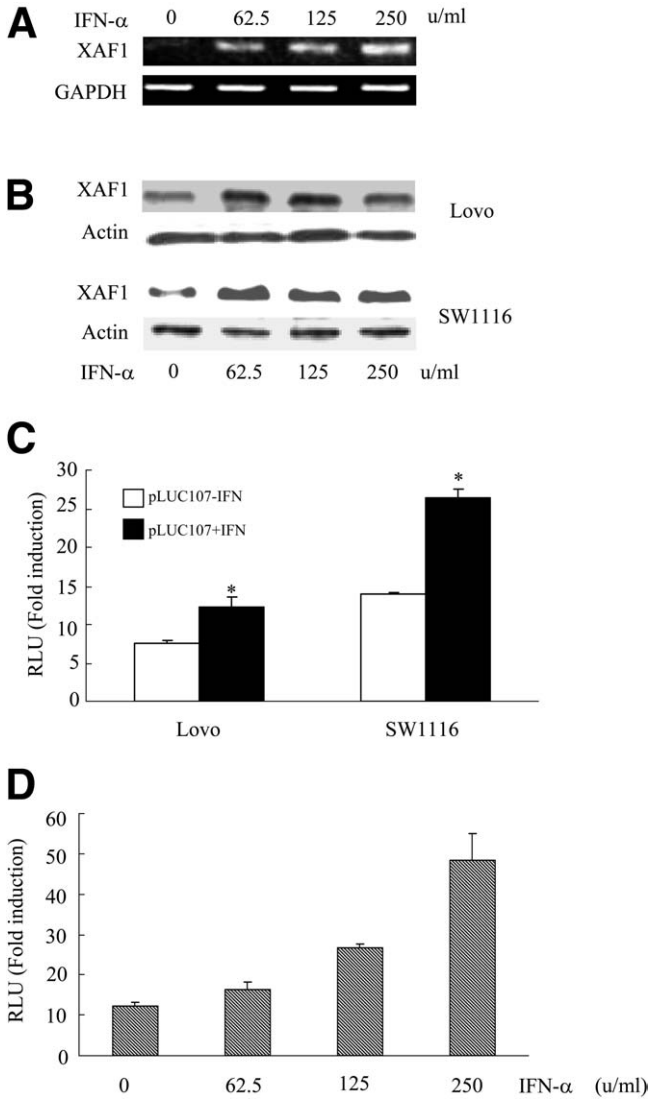

Figure 1. Identification of XAF1 as an ISG. (*A*) SW1116 cells were treated with 62.5, 125, and 250 U of IFN-alfa for 24 hours. XAF1 mRNA expression was detected by reverse-transcription PCR. (*B*) Lovo and SW1116 cells were treated with IFN-alfa for 48 hours. XAF1 protein expression was detected by immunoblotting. Glyceraldehyde-3-phosphate dehydrogenase and actin were used as the internal controls. These figures are representative of 3 independent experiments with consistent findings. (*C*) Lovo and SW1116 cells transfected with pLUC107 were treated with or without 125 U/mL of IFN-alfa. Luciferase activities were measured 48 hours later. $*P < .05$ compared with untreated control. (*D*) SW1116 cells transfected with pLUC107 were treated with various concentrations of IFN-alfa. Luciferase activities were assayed 48 hours later. Promoter activity was presented as the fold induction of the RLU compared with basic pGL3 vector control. All results are expressed as the mean of 3 independent experiments ± SD.

clear extract with IRF-E–XAF1 probe. We found that consensus IRF-1 probe blocked the binding completely (Figure 2*D*). These results inferred the existence of a high-affinity IRF-E sequence in the 5′-flanking region of XAF1 gene.

Site-Directed Mutation of IRF-E Abrogated IFN-Induced XAF1 Promoter Activity

To clarify the function of the putative IRF-E sequence further, we generated 2 site-directed mutation constructs. One mutation site was outside of the IRF-E region (-28 nt), and another was located at the center of the IRF-E element (-34 nt). Dual luciferase reporter assay

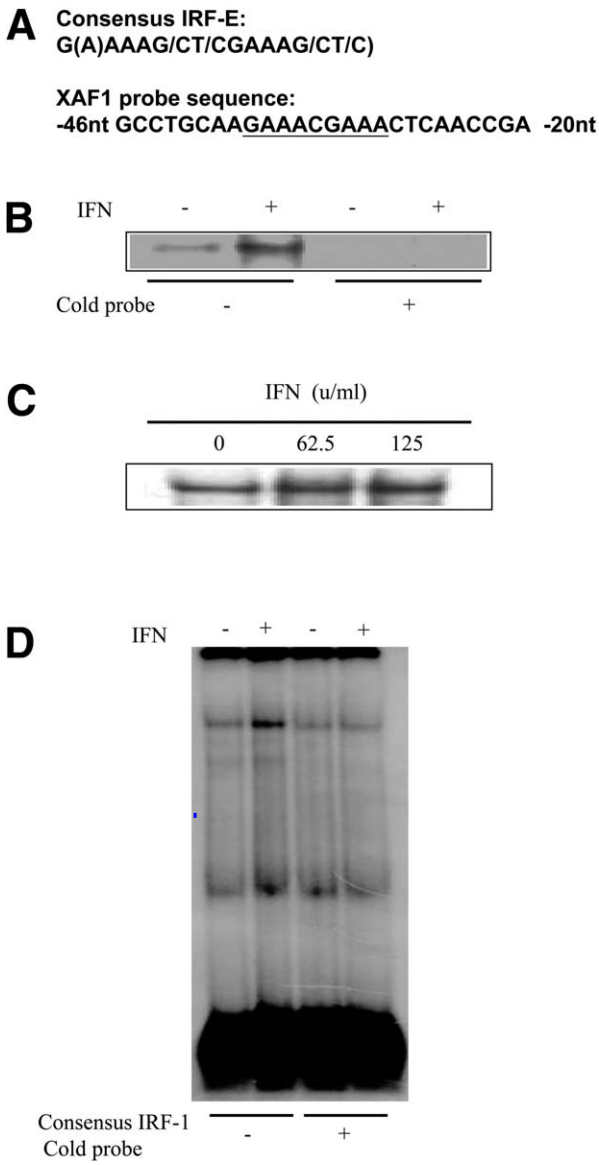

Figure 2. Identification of a high-affinity IRF-E in the transcription starting site of XAF1. (*A*) List of consensus IRF-1 sequence and analysis of a putative IRF-E sequence within the XAF1 promoter. The upstream nucleotide adjacent to the translation initiator ATG codon was defined as –1. (*B*, *C*) SW1116 cells treated with IFN-alfa for 12 hours were subjected to an EMSA to check the binding to ^{32}P-labeled IRF-E–XAF probe. Excessive amount of unlabeled probe was used as cold probe. (*D*) Nuclear protein of SW1116 cells with or without IFN-alfa (62.5 U/mL) treatment were extracted and bound to IRF-E–XAF probe. Excessive amount of nonlabeled IRF-1 consensus probe was used as cold probe. These figures are representative of 2 independent experiments.

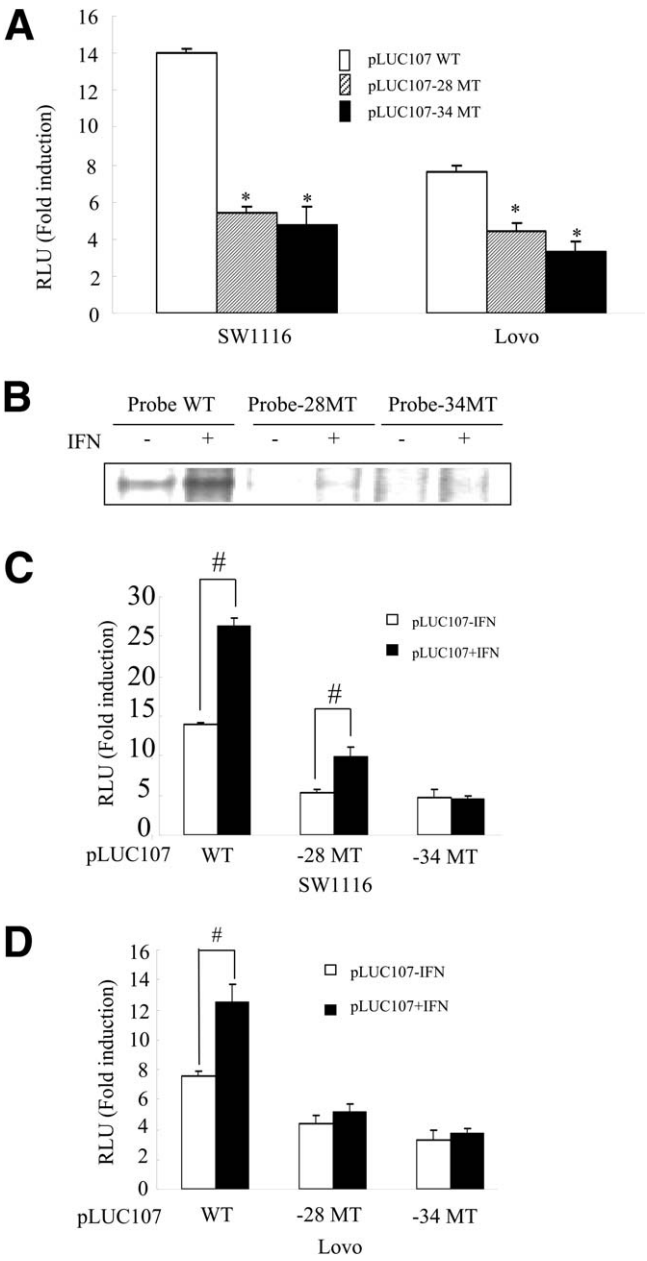

Figure 3. Site-directed mutation of IRF-E abrogates IFN-induced promoter activity. (*A*) SW1116 and Lovo cells were transfected with wild-type (WT), –28 nt, or –34 nt mutant (MT) pLUC107 constructs and were assayed for luciferase activity 48 hours later. $*P < .05$ compared with WT. Fold induction of RLU was expressed as the mean of 4 independent experiments ± SD. (*B*) Nuclear extract of SW1116 cells was bound to ^{32}P-labeled WT, –28 nt, and –34 nt MT probes in an EMSA assay. This experiment was repeated twice with the same results. (*C, D*) SW1116 and Lovo cells transfected with WT, –28 nt, and –34 nt MT pLUC107 constructs were treated with or without IFN-alfa and assayed for luciferase activities 48 hours later ($\#P < .05$). These experiments were repeated 3 times with the same results. Fold inductions of RLU were expressed as the mean of 3 independent experiments ± SD.

showed that the transcription activities of both mutated constructs were lower than that of the wild-type control (Figure 3*A*, $P < .05$). The transcription activities of wild-type, –28 mutant, and –34 mutant pLUC107 constructs were 7.6 ± .3, 4.4 ± .5, and 3.3 ± .6, respectively, in Lovo cells, and 14 ± .2, 5.4 ± .3, and 4.8 ± .9 in SW1116 cells. These results indicated that both sites were important in maintaining effective transcription activity of XAF1. An EMSA assay showed that both site mutations eliminated the intrinsic and IFN-induced binding to IRF-E–XAF1 probe (Figure 3*B*). Regarding the transcription response to IFN-alfa, as shown in Figure 3*C* and *D*, –28 nt site mutation did not or only slightly eliminated the effect of IFN-alfa in both SW1116 and Lovo cells. However, –34 site mutation abrogated the effect of IFN-alfa completely. The transcription activity of –34 mutant pLUC107 construct without or with IFN treatment was 3.3 ± .6 vs 3.7 ± .4 in Lovo cells and 4.8 ± .9 vs 4.6 ± .4 in SW1116 cells, respectively ($P > .05$ for both cell lines), suggesting that IRF-E–XAF1 conferred IFN-induced XAF1 transcription.

ATRA Up-Regulated XAF1 Expression

To examine further if ATRA can up-regulate XAF1 transcription, we first treated Lovo and SW1116 cells with various concentrations of ATRA. We showed that XAF1 expression was up-regulated significantly (Figure 4*A*, *B*). We next transfected pLUC107 constructs into cells followed by treatment with 16.5 μmol/L of ATRA. The transcription activity of pLUC107 without and with ATRA treatment was 7 ± .5 vs 19 ± .7 and 15 ± 1.2 vs 29 ± 2.5 for Lovo and SW1116 cells, respectively (Figure 4*C*, $P < .05$), suggesting that ATRA increased XAF1 expression via transcriptional regulation.

IRF-E Mediated ATRA-Induced XAF1 Expression

To elucidate the role of IRF-E in ATRA-induced XAF1 expression, we first checked the binding capacity of IRF-E–XAF1 probe in the presence or absence of ATRA. We showed that ATRA increased the specific binding of IRF-E–XAF1 probe significantly (Figure 5*A*). Second, we examined the activity of IRF-E–XAF1 in vivo by chromatin-immunoprecipitation assay using specific antibody against IRF-1. Normal rabbit IgG was used as the negative control. DNA associated with the chromatin immunoprecipitated by these antibodies then was amplified by PCR with primers specific for the IRF-E region of XAF1 promoter (–141/+30). As expected, no DNA fragments were detected when normal IgG was used (Figure 5*B*, lanes 2, 5, and 8). In contrast, DNA fragments with the expected size were detected using anti–IRF-1 antibody in Lovo (Figure 5*B*) and SW1116 cells (data not shown). In addition, we showed

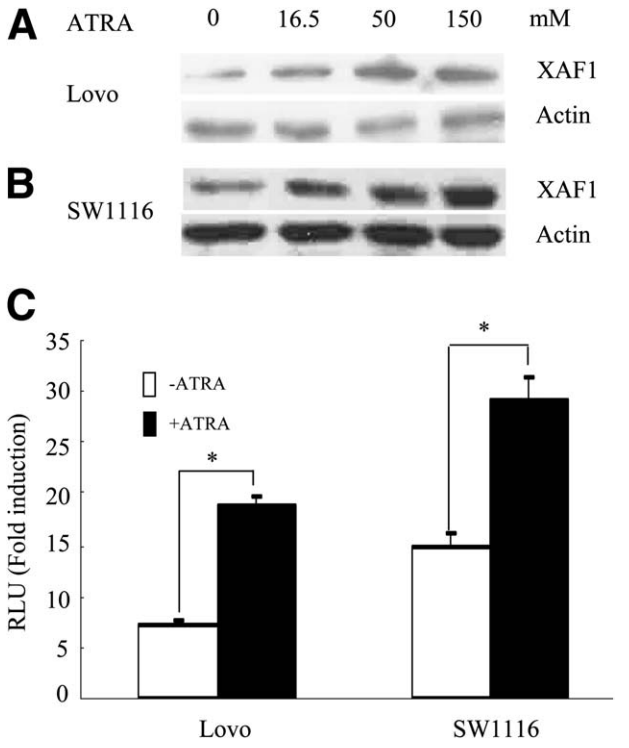

Figure 4. ATRA up-regulated XAF1 transcription. (*A*, *B*) Lovo and SW1116 cells were treated with 16.5, 50, and 150 μmol/L of ATRA, XAF1 expression was detected 48 hours later by immunoblotting. Actin was used as internal control. These figures were representative of 3 independent experiments with identical results. (*C*) Lovo and SW1116 cells transfected with pLUC107 construct were treated with 16.5 μmol/L of ATRA for 48 hours. Luciferase activities were measured ($*P < .05$). Fold induction of RLU was expressed as the mean of 3 independent experiments ± SD.

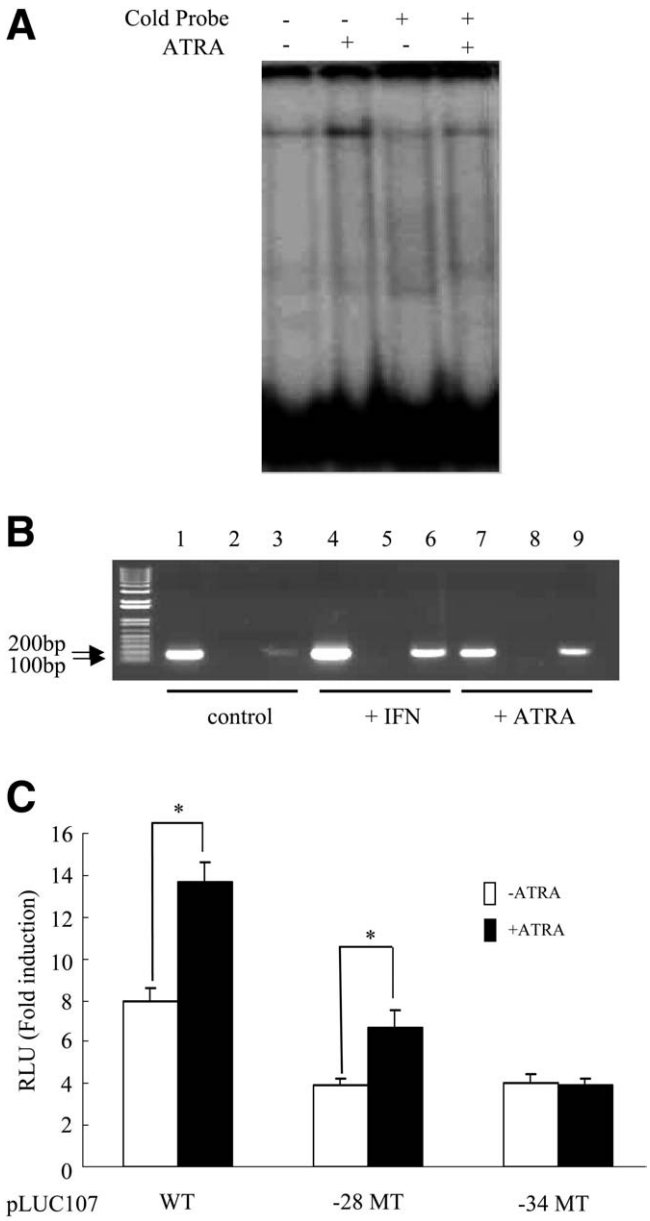

Figure 5. IRF-E mediated ATRA-induced XAF1 expression. (*A*) SW1116 cells were treated with dissolvent or 16.5 μmol/L of ATRA for 12 hours. Nuclear extracts were prepared to detect the binding to ^{32}P-labeled IRF-E–XAF1 probe. This experiment was repeated twice with the same results. (*B*) Chromatin immunoprecipitation analysis of IRF-E–XAF1 element from untreated (lanes 1–3), IFN-alfa (62.5 u, lanes 4–6), and ATRA (16.5 μmol/L, lanes 7–9) induced (24 h) Lovo cells using antibody specific for IRF-1 (lanes 3, 6, 9) or rabbit IgG control (lanes 2, 5, 8). Input chromatins are shown in lanes 1, 4, and 7. This experiment was repeated twice in both Lovo and SW1116 cells with similar results. (*C*) Wild-type (WT), –28 nt, and –34 nt mutant (MT) pLUC107 constructs were transfected into SW1116 cells for 8 hours, followed by treatment with dissolvent control or 16.5 μmol/L ATRA for an additional 48 hours and luciferase activity was measured. $*P < .05$. These experiments were repeated in both SW1116 and Lovo cells with consistent results. Fold induction of RLU was expressed as the mean of 3 independent experiments ± SD.

that pretreatment with IFN-alfa and ATRA increased the amount of immunoprecipitated DNA (Figure 5*B*). This finding showed that IRF-E–XAF1 and IRF-1 formed a complex at the XAF1 promoter to regulate XAF1 transcription positively. Third, we transfected wild-type, –28 nt, and –34 nt mutated pLUC107 constructs into SW1116 cells and measured the luciferase activities. As shown in Figure 5*C*, –34 nt mutation but not the –28 nt mutation abrogated ATRA-induced transcription activity of pLUC107. These findings suggested that IRF-E–XAF1 contributed to ATRA-induced XAF1 expression.

Suppression of IRF-1-Abrogated ATRA-Induced XAF1 Expression

To confirm further the role of IRF-1 in ATRA-induced XAF1 expression, we synthesized specific IRF-1 siRNA. Its effect in suppressing IRF-1 expression was verified by immunoblotting assay (Figure 6*A*). We then transfected Lovo cells with control (GL2) or IRF-1 siRNA and exposed the cells to ATRA subsequently. An

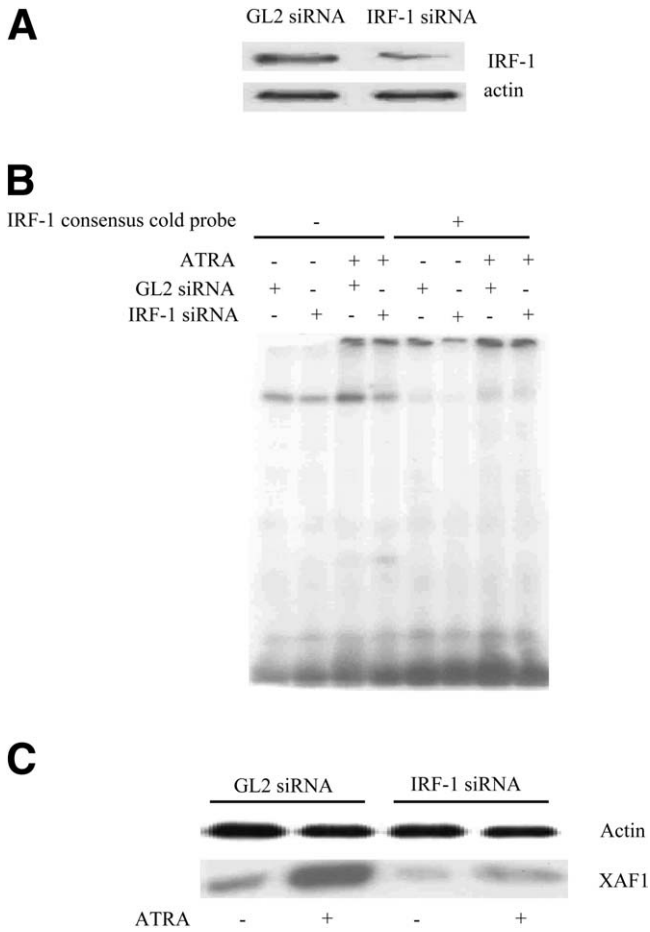

Figure 6. Suppression of IRF-1 abrogated ATRA-induced XAF1 expression. (*A*) Lovo cells were transfected with control (GL2) or IRF-1 siRNA for 48 hours. IRF-1 expression was detected by immunoblotting with actin as the internal control. This experiment was repeated twice in both Lovo and SW1116 cells with identical results. (*B*) Lovo cells were transfected with GL2 or IRF-1 siRNA for 48 hours followed by treatment with dissolvent or 16.5 μmol/L of ATRA for 12 hours. Nuclear extracts were prepared to detect the binding to ^{32}P-labeled IRF-E–XAF1 probe in the presence or absence of consensus IRF-1 cold probe. This experiment was repeated twice in both Lovo and SW1116 cells with similar findings. (*C*) Lovo cells were transfected with GL2 or IRF-1 siRNA for 48 hours followed by treatment with dissolvent or 16.5 μmol/L of ATRA for an additional 48 hours. XAF1 expression was detected by immunoblotting. This figure is representative of 3 independent experiments with identical results.

EMSA assay showed that suppression of IRF-1 eliminated the binding capacity of IRF-E–XAF1 (Figure 6*B*). Finally, we showed that suppression of IRF-1 through RNA interference abrogated ATRA-induced XAF1 expression. These findings further implicated the role of IRF-1/IRF-E–XAF1 complex in ATRA-induced XAF1 expression.

XAF1 Participated in ATRA-Induced Cell-Growth Suppression

To define the significance of ATRA-induced XAF1 expression, we examined the role of XAF1 in ATRA-mediated suppression of cancer cell growth. We transfected Lovo and SW1116 cells with pcDNA empty vector, XAF1-S, and XAF1-AS transiently, followed by ATRA treatment. Cell proliferation was evaluated by MTT assay. As shown in Figure 7*A*, proliferation of Lovo cells transfected with empty vector, XAF-S, and AS were 85.8% ± 4%, 52.98% ± 2%, and 90.66% ± 1%, respectively, whereas that for SW1116 cells were 86.24% ± 1%, 65.29% ± 2%, and 108.29% ± 2%, respectively. It indicated that overexpression of XAF1 increased cell susceptibility to ATRA-mediated growth suppression ($P < .05$) in both Lovo and SW1116 cells. The suppression of XAF1 by transfection with antisense construct reversed the effect of ATRA significantly or completely ($P > .05$ for Lovo cells and $<.05$ for SW1116 cells).

We established that Lovo cell transfectants stably expressed vector control (Lovo/vector), XAF1 sense (Lovo/XAF1-S), and XAF1 antisense (Lovo/XAF1-AS). XAF1 expression was confirmed by immunoblotting (Figure 7*B*). The response of stable transfectants to ATRA was evaluated. As shown in Figure 7*C*, the susceptibility to ATRA-induced growth inhibition was higher in Lovo/XAF-S than that of Lovo/vector. In contrast, Lovo/XAF-AS was resistant to ATRA-induced growth suppression with the inhibition rate only around 10% even at the highest ATRA concentration.

ATRA-Induced XAF1 Expression In Vivo

To validate the effect of ATRA on XAF1 expression in vivo, we inoculated Lovo/vector and Lovo/XAF1-S stable transfectants into BALB/c-*nu*/*nu* mice and treated them with ATRA after the formation of tumors. ATRA suppressed tumor growth significantly compared with vehicle control (Figure 8*A*1, *A*2, and *B*; $P < .05$). The growth rate of Lovo/XAF1-S transfectant was significantly slower than that of Lovo/vector (Figure 8*A*1, *A*3, and *B*; $P < .05$). In addition, overexpression of XAF1 generated a synergized effect with ATRA in suppressing tumor cell growth (Figure 8*A*, *B*; $P < .05$). In fact, 3 of 4 tumors formed by Lovo/XAF1-S transfectant were eliminated completely by ATRA (Figure 8*A*4). We then detected XAF1 expression in tumor tissues derived from Lovo/vector transfectant with or without ATRA treatment. As shown in Figure 8*C*, ATRA induced XAF1 expression in all mice. These findings confirmed the in vitro findings that ATRA induced XAF1 expression in colon cancer cells and XAF1 participated in ATRA-induced growth suppression.

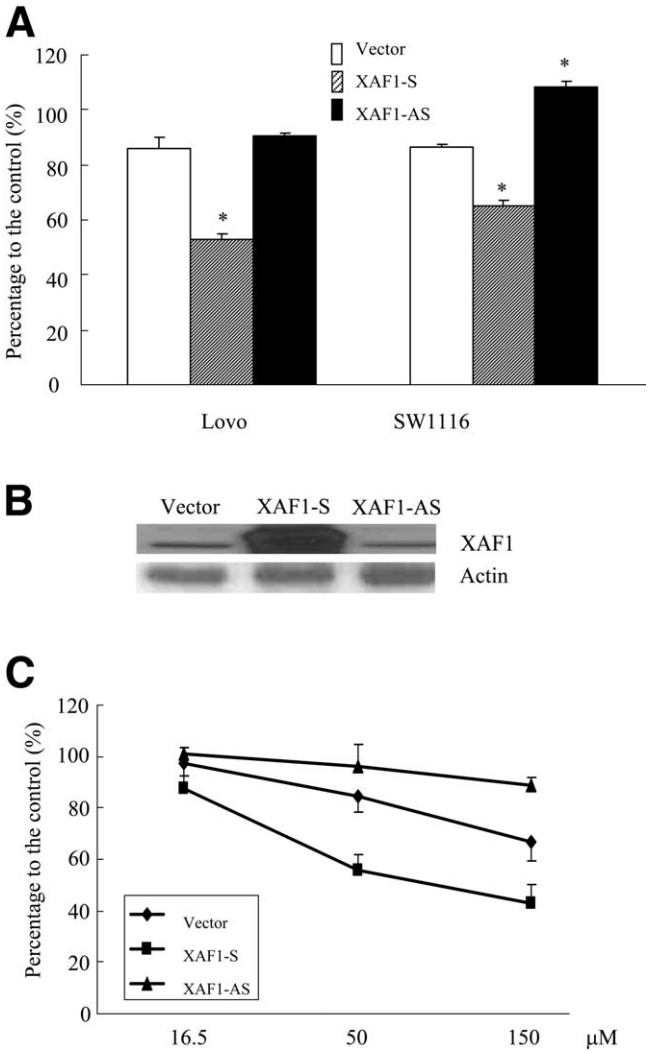

Figure 7. XAF1 participated in ATRA-induced cell growth suppression. (*A*) Lovo and SW1116 cells were transfected with pCDNA empty vector, XAF1-S, and XAF1-AS construct for 8 hours, followed by the treatment with dissolvent control or 150 μmol/L of ATRA for 48 hours. Cell proliferation was evaluated by MTT assay and expressed as a percentage to dissolvent control. $*P < .05$ compared with vector control. (*B*) XAF1 expression of Lovo/vector, Lovo/XAF1-S, and Lovo/XAF1-AS stable transfectants were detected by immunoblotting. Actin was used as internal control. This figure is representative of 2 independent experiments with identical results. (*C*) Stable transfectants of Lovo/vector, Lovo/XAF1-S, and Lovo/XAF1-AS were seeded into 96-well plates and exposed to 16.5, 50, and 150 μmol/L of ATRA for 48 hours. Cell proliferation was evaluated by MTT assay. All results were expressed as the mean of 3 independent experiments ± SD.

ATRA-Induced XAF1 Expression Was Independent of the Translocation of XIAP and Methylation of XAF1 Promoter

Liston et al[7] reported that overexpression of XAF1 triggered a redistribution of XIAP from the cytosol to nucleus, whereas Leaman et al[10] reported that IFN treatment did not alter the subcellular distribution of XAF1 and XIAP. To test the effect of ATRA, we transfected Lovo cells with RFP-XAF1 and GFP-XIAP constructs. We showed that XIAP was located predominantly in the cytosol. Treatment with ATRA did not induce nuclear translocation of XIAP (Figure 9*A*1, *A*2). In contrast, XAF1 was located mainly in the nucleus (Figure 9*A*3, and *A*4). Treatment with ATRA did not alter its subcellular localization either. Next, we extracted the cytosolic and nuclear fractions of Lovo cells for detection of XIAP and XAF1. Consistent with the earlier-described findings, XIAP accumulated in the cytosol and XAF1 was

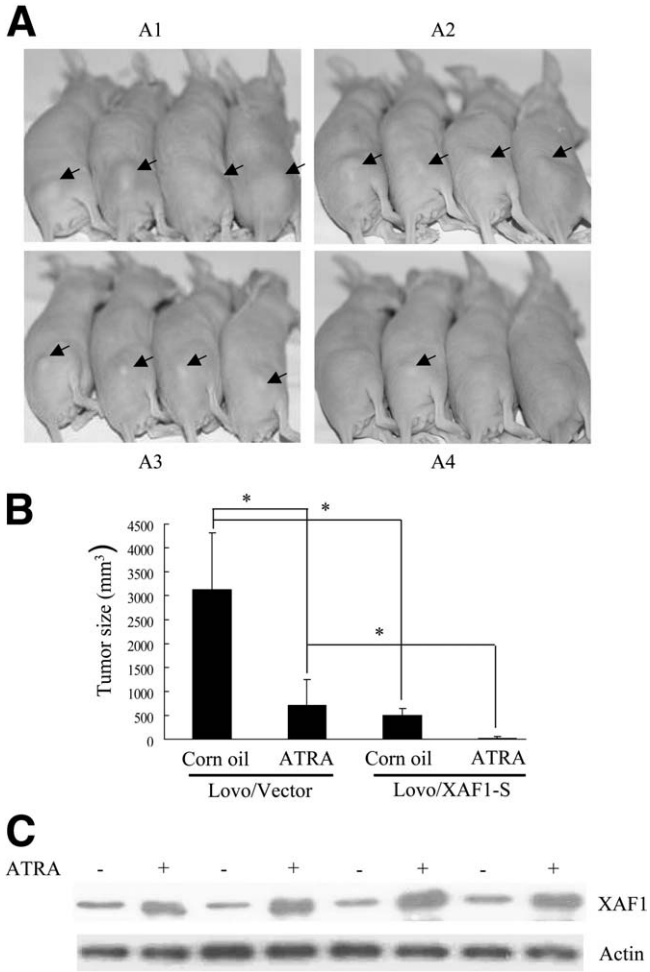

Figure 8. ATRA induced XAF1 expression in vivo. (*A*) Tumor formation in mice inoculated with Lovo/vector (A1 and A2) and Lovo/XAF1 (A3 and A4) transfectants and treated with vehicle control (corn oil, A1 and A3) or ATRA (A2 and A4). (*B*) Tumor size of mice with different treatments. The volumes of tumor were calculated as follows: $V = (4/3)\ R1^2\ R2$, where $R1$ is radius 1 and $R2$ is radius 2 and $R1 < R2$. Data were the pooled average ± SD of the tumor volumes for each of 4 animals per group, repeated twice. $*P < .05$. (*C*) XAF1 expression in xenograft samples. Tumors derived from mice inoculated with Lovo/vector and treated without (A1) or with ATRA (A2) were excised and lysed. Expression of XAF1 was detected by immunoblotting. This figure is representative of 2 independent experiments with similar results.

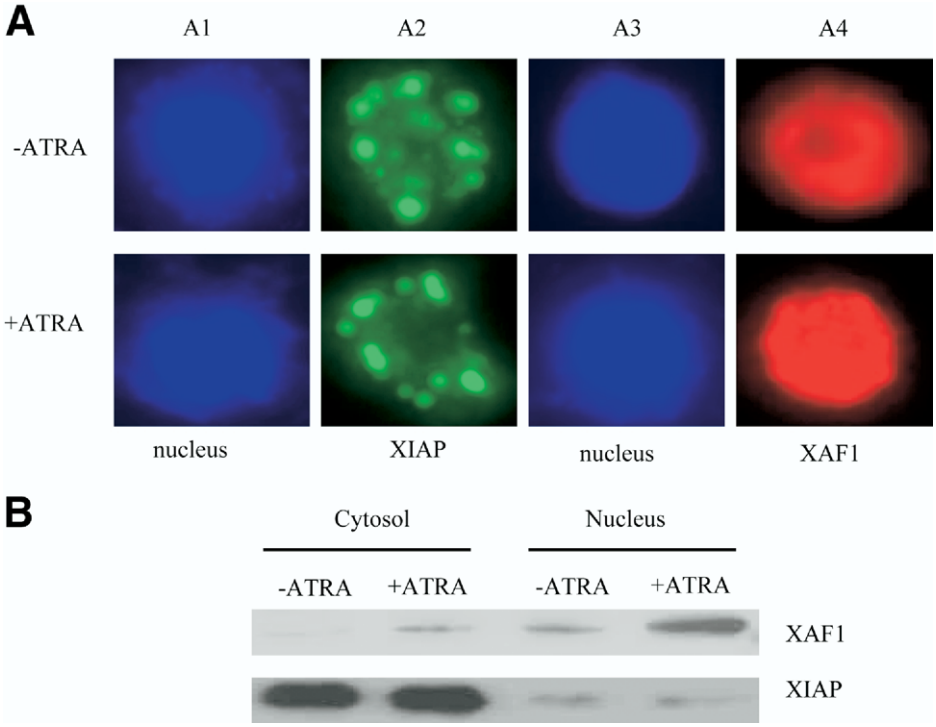

Figure 9. ATRA did not alter the location of XAF1 and XIAP. (*A*) Lovo cells were transfected with pDs-red2-c1-XAF1 and pEGFP-C1-XIAP separately for 12 hours, followed by treatment with ATRA (150 μmol/L) for 48 hours. The locations of XAF1 (*red*) and XIAP (*green*) were observed under a fluorescent microscope after counterstaining with Hoechst 22358 (*blue*) for 10 minutes. (*B*) Cytosolic and nuclear extracts of Lovo cells with or without ATRA treatment (150 μmol/L) for 48 hours were prepared. The expressions of XAF1 and XIAP were detected by immunoblotting. These figures were representatives of 2 independent experiments.

localized at the nucleus with no changes after ATRA treatment (Figure 8*B*).

To test if ATRA up-regulated XAF1 expression through demethylation of the promoter, we first searched the whole genomic DNA sequence of XAF1 using the Methprimer technology (University of California, San Francisco [UCSF]) (http://www.urogene.org/methprimer) and found that the XAF1 gene was not enriched in CpG dinucleotides. There were some small clusters of CpG sites in whole genomic DNA that did not fulfill the criteria for CpG islands. Similar to the findings by Byun et al[8] that the proximal CpG site methylation correlated with the silencing of XAF1 transcription, we found 8 CpG sites in the 5′ proximal region and exon 1 (nt −59 to +194). They were located at −33/−34, −22/−23, 17/18, 54/55, 63/64, 71/72, 82/83, and 88/89, respectively. The sequence region spanning these 8 CpG sites was amplified by PCR using sodium bisulfite–modified DNA as templates, and 10 PCR clones were sequenced to determine methylation frequency at individual CpG sites (complete methylation, 70%–100%; partial methylation, 10%–60%; unmethylation, 0%). The results showed that no methylation occurred in 17 of 18 and 63 of 64 CpG sites in both Lovo and SW1116 cells, respectively. Partial or complete methylation was found in other CpG sites in both cell lines. Treatment with ATRA did not alter the methylation status of these CpG sites.

Discussion

In this report, we provided several novel results important for understanding the role and mechanism of XAF1 in tumor cell growth. XAF1 was modulated positively by ATRA and IFN through an IRF-E–mediated transcription regulation and participated in ATRA-induced cell-growth inhibition.

XAF1 has been classified as an ISG in melanoma cells with mechanisms unknown.[10,11] Our results confirmed this observation in colon cancer cell lines. In addition, we successfully identified a high-affinity and functional IRF-E in the proximal promoter of the XAF1 gene, suggesting that IFN induced XAF1 expression directly through transcription regulation. The IRF-E we identified was influential in regulating XAF1 transcription because it was located close to or within the transcription starting area of the XAF1 gene. We have identified the transcription starting site of the XAF1 gene that is located at −26 nt (adenosine) by a 5′-RACE assay (unpublished data). Through searching the database transcription starting site database (http://dbtss.hgc.jp/index.html) in which most genes possessed multiple transcription starting sites, we found that the XAF1 transcription starting region was located at −4 to −40 nt. Site-directed mutagenesis of both −28 and −34 nt down-regulated the transcription activity of pLUC107 significantly, supporting the importance of this region in keeping XAF1 transcription activity.

IFNs are the first family of human proteins to be effective in cancer therapy and are among the first recombinant DNA products to be used clinically.[26] IFNs mediate antitumor effects either indirectly by modulating immunomodulatory and antiangiogenic responses or directly by affecting proliferation or cellular differentiation of tumor cells.[27–30] Similar to IFN, RA exerts profound influences on cell growth and differentiation.[16–18,31–33] Several in vitro studies have shown that the combined administration of RAs and IFNs leads to a modulation in the expression of some ISGs and an increased inhibition of cell proliferation.[34,35]

One candidate mechanism for the cross-talk between RA and IFN is the up-regulation of IRF-1.[35–40] RA is capable of up-regulating IRF-1 expression in heterologous cancer cell types including myeloid leukemia, acute promyelocytic leukemia, cervical squamous cancer, and breast cancer cells,[17–19,34,35] resulting in both the induction of IFNs and ISGs.[25,28] Our finding suggests that XAF1 is not only an ISG, but also an effector in mediating the synergized antitumor effect of IFNs and RA.

Because RA-dependent up-regulation of IRF-1 apparently is not mediated by the classic pathway involving nuclear RA receptor,[17,37,38] the induction of IRF-1 requires a high dose of ATRA. It has been observed that ATRA dose-dependently suppressed the growth of cervical carcinoma cells. The suppression of growth required sustained activation of IRF-1, which was achieved by high-dose (10^{-4} mol/L) but not low-dose (10^{-6} mol/L) of ATRA.[36] A low dose of ATRA only can induce transient up-regulation of IRF-1. We consistently found that although a lower dose of ATRA (16.5 μmol/L) suppressed the growth of Lovo/XAF1 stable transfectant (Figure 7*C*), only a higher dose (50 μmol/L and 150 μmol/L) of ATRA suppressed tumor cell growth significantly when transfected with XAF1 transiently (Figure 7*A* and data not shown). Thinking about the low transfection efficiency of transient transfection (5%–15%), this finding indicated that both the induction of IRF-1 expression and overexpression of XAF1 are important in mediated ATRA-induced cell growth suppression, suggesting XAF1 as a prevailing effector of ATRA. This notion was confirmed further by an in vivo tumorigenicity experiment.

As a tumor suppressor, overexpression of XAF1 increased cell susceptibility to etoposide and tumor necrosis factor–related apoptosis inducing ligand-induced apoptosis. Similarly, it increased ATRA-induced apoptosis identified by DAPI staining (data not shown). The only well-defined function pathway of XAF1 antagonizes the effect of XIAP. However, we cannot confirm the findings of Liston et al[7] that overexpression of XAF1 sequestered XIAP to the nucleus. Our result was consistent with the report by Leaman et al[10] that IFN up-regulated XAF1 expression without altering the localization of both XIAP and XAF1 proteins. It suggested that XAF1 might mediate ATRA-induced cell growth suppression in a mechanism other than interaction with XIAP. In fact, as an ISG, tumor necrosis factor–related apoptosis inducing ligand expression also could be up-regulated by both RA and IFNs in cancer cells.[39,40] Thus, overexpression of XAF1 might increase cell susceptibility to tumor necrosis factor–related apoptosis inducing ligand or other ISG-induced apoptosis. This hypothesis remains to be clarified in the future.

In conclusion, a high affinity of IRF-E close to the transcription starting site mediated IFN- and ATRA-induced XAF1 expression. XAF1 participated in ATRA-induced cell-growth suppression that might be independent of the interaction with XIAP, implicating XAF1 to be a putative target in the combined therapy of colon cancer.

References

1. LaCasse EC, Baird S, Korneluk RG, MacKenzie AE. The inhibitors of apoptosis (IAPs) and their emerging role in cancer. Oncogene 1998;17:3247–3259.
2. Holcik M, Gibson H, Korneluk RG. XIAP: apoptotic brake and promising therapeutic target. Apoptosis 2001;6:253–261.
3. Ferreira CG, van der Valk P, Span SW, Jonker JM, Postmus PE, Kruyt FA, Giaccone G. Assessment of IAP (inhibitor of apoptosis) proteins as predictors of response to chemotherapy in advanced non-small-cell lung cancer patients. Ann Oncol 2001;12:799–805.
4. Chawla-Sarkar M, Bae SI, Reu FJ, Jacobs BS, Lindner DJ, Borden EC. Downregulation of Bcl-2, FLIP or IAPs (XIAP and survivin) by siRNAs sensitizes resistant melanoma cells to Apo2L/TRAIL-induced apoptosis. Cell Death Differ 2004;11:915–923.
5. Bilim V, Kasahara T, Hara N, Takahashi K, Tomita Y. Role of XIAP in the malignant phenotype of transitional cell cancer (TCC) and therapeutic activity of XIAP antisense oligonucleotides against multidrug-resistant TCC in vitro. Int J Cancer 2003;103:29–37.
6. Fong WG, Liston P, Rajcan-Separovic E, St Jean M, Craig C, Korneluk RG. Expression and genetic analysis of XIAP-associated factor 1 (XAF1) in cancer cell lines. Genomics 2000;70:113–122.
7. Liston P, Fong WG, Kelly NL, Toji S, Miyazaki T, Conte D, Tamai K, Craig CG, McBurney MW, Korneluk RG. Identification of XAF1 as an antagonist of XIAP anti-Caspase activity. Nat Cell Biol 2001;3:128–133.
8. Byun DS, Cho K, Ryu BK, Lee MG, Kang MJ, Kim HR, Chi SG. Hypermethylation of XIAP-associated factor 1, a putative tumor suppressor gene from the 17p13.2 locus, in human gastric adenocarcinomas. Cancer Res 2003;63:7068–7075.
9. Ma TL, Ni PH, Zhong J, Tan JH, Qiao MM, Jiang SH. Low expression of XIAP-associated factor 1 in human colorectal cancers. Chin J Dig Dis 2005;6:10–14.
10. Leaman DW, Chawla-Sarkar M, Vyas K, Reheman M, Tamai K, Toji S, Borden EC. Identification of X-linked inhibitor of apoptosis-associated factor-1 as an interferon-stimulated gene that aug-

ments TRAIL Apo2L-induced apoptosis. J Biol Chem 2002;277:28504–28511.
11. Leaman DW, Chawla-Sarkar M, Jacobs B, Vyas K, Sun Y, Ozdemir A, Yi T, Williams BR, Borden EC. Novel growth and death related interferon-stimulated genes (ISGs) in melanoma: greater potency of IFN-beta compared with IFN-alpha2. J Interferon Cytokine Res 2003;23:745–756.
12. Chanchevalap S, Nandan MO, Merlin D, Yang VW. All-trans retinoic acid inhibits proliferation of intestinal epithelial cells by inhibiting expression of the gene encoding Kruppel-like factor 5. FEBS Lett 2004;578:99–105.
13. Stewart LV, Thomas ML. Retinoids differentially regulate the proliferation of colon cancer cell lines. Exp Cell Res 1997;233: 321–329.
14. Naka K, Yokozaki H, Domen T, Hayashi K, Kuniyasu H, Yasui W, Lotan R, Tahara E. Growth inhibition of cultured human gastric cancer cells by 9-cis-retinoic acid with induction of cdk inhibitor Waf1/Cip1/Sdi1/p21 protein. Differentiation 1997; 61:313–320.
15. Ohno S, Nishi T, Kojima Y, Haraoka J, Ito H, Mizuguchi J. Combined stimulation with interferon alpha and retinoic acid synergistically inhibits proliferation of the glioblastoma cell line GB12. Neurol Res 2002;24:697–704.
16. Nanus DM, Geng Y, Shen R, Lai HK, Pfeffer SR, Pfeffer LM. Interaction of retinoic acid and interferon in renal cancer cell lines. J Interferon Cytokine Res 2000;20:787–794.
17. Percario ZA, Giandomenico V, Fiorucci G, Chiantore MV, Vannucchi S, Hiscott J, Affabris E, Romeo G. Retinoic acid is able to induce interferon regulatory factor 1 in squamous carcinoma cells via a STAT-1 independent signalling pathway. Cell Growth Differ 1999;10:263–270.
18. Mahon FX, Chahine H, Barbot C, Pigeonnier V, Jazwiec B, Reiffers J, Ripoche J. All-trans retinoic acid potentiates the inhibitory effects of interferon alpha on chronic myeloid leukemia progenitors in vitro. Leukemia 1997;11:667–673.
19. Clarke N, Jimenez-Lara AM, Voltz E, Gronemeyer H. Tumor suppressor IRF-1 mediates retinoid and interferon anticancer signaling to death ligand TRAIL. EMBO J 2004;23:3051–3060.
20. Jiang XH, Tu SP, Cui JT, Lin MC, Xia HH, Wong WM, Chan AO, Yuen MF, Jiang SH, Lam SK, Kung HF, Soh JW, Weinstein IB, Wong BC. Antisense targeting protein kinase C alpha and beta1 inhibits gastric carcinogenesis. Cancer Res 2004;64: 5787–5794.
21. Tu SP, Jiang XH, Lin MC, Cui JT, Yang Y, Lum CT, Zou B, Zhu YB, Jiang SH, Wong WM, Chan AO, Yuen MF, Lam SK, Kung HF, Wong BC. Suppression of survivin expression inhibits in vivo tumorigenicity and angiogenesis in gastric cancer. Cancer Res 2003;63: 7724–7732.
22. Wong BC, Jiang XH, Lin MC, Tu SP, Cui JT, Jiang SH, Wong WM, Yuen MF, Lam SK, Kung HF. Cyclooxygenase-2 inhibitor (SC-236) suppresses activator protein-1 through c-Jun NH2-terminal kinase. Gastroenterology 2004;126:136–147.
23. Shalinsky DR, Bischoff ED, Gregory ML, Gottardis MM, Hayes JS, Lamph WW, Heyman RA, Shirley MA, Cooke TA, Davies PJ. Retinoid-induced suppression of squamous cell differentiation in human oral squamous cell carcinoma xenografts (line 1483) in athymic nude mice. Cancer Res 1995;55:3183–3191.
24. Pettersson F, Colston KW, Dalgleish AG. Retinoic acid enhances the cytotoxic effects of gemcitabine and cisplatin in pancreatic adenocarcinoma cells. Pancreas 2001;23:273–279.
25. Tanaka N, Kawakami T, Taniguchi T. Recognition DNA sequences of interferon regulatory factor 1 (IRF-1) and IRF-2, regulators of cell growth and the interferon system. Mol Cell Biol 1993;13:4531–4538.
26. Wadler S. The role of interferons in the treatment of solid tumors. Cancer 1992;70(Suppl):949–958.
27. Fujita T, Sakakibara J, Sudo Y, Miyamoto Fujita T, Kimura Y, Miyamoto M, Barsoumian EL, Taniguchi T. Induction of endogenous IFN-α and IFN-β genes by a regulatory transcription factor, IRF-1. Nature 1989;337:270–272.
28. Chawla-Sarkar M, Lindner DJ, Liu YF, Williams BR, Sen GC, Silverman RH, Borden EC. Apoptosis and interferons: role of interferon-stimulated genes as mediators of apoptosis. Apoptosis 2003;8:237–249.
29. Baghdiguian S, Verrier B, Roccabianca M, Pommier G, Marvaldi J, Fantini J. Vectorial release of carcinoembryonic antigen induced by IFN-gamma in human colon cancer cells cultured in serum-free medium. Eur J Cancer 1991;27:599–604.
30. Wong VL, Rieman DJ, Aronson L, Dalton BJ, Greig R, Anzano MA. Growth-inhibitory activity of interferon-beta against human colorectal carcinoma cell lines. Int J Cancer 1989;43:526–530.
31. Zhang JW, Wang JY, Chen SJ, Chen Z. Mechanisms of all-trans retinoic acid-induced differentiation of acute promyelocytic leukemia cells. J Biosci 2000;25:275–284.
32. Smith MA, Parkinson DR, Cheson BD, Friedman MA. Retinoids in cancer therapy. J Clin Oncol 1992;10:839–864.
33. Dawson MI, Zhang XK. Discovery and design of retinoic acid receptor and retinoid X receptor class- and subtype-selective synthetic analogs of all-trans-retinoic acid and 9-cis-retinoic acid. Curr Med Chem 2002;9:623–637.
34. Lingen MW, Polverini PJ, Bouck NP. Retinoic acid and interferon alpha act synergistically as antiangiogenic and antitumor agents against human head and neck squamous cell carcinoma. Cancer Res 1998;58:5551–5558.
35. Um SJ, Kim EJ, Hwang ES, Kim SJ, Namkoong SE, Park JS. Antiproliferative effects of retinoic acid/interferon in cervical carcinoma cell lines: cooperative growth suppression of IRF-1 and p53. Int J Cancer 2000;85:416–423.
36. Arany I, Whitehead WE, Grattendick KJ, Ember IA, Tyring SK. Suppression of growth by all-trans retinoic acid requires prolonged induction of interferon regulatory factor 1 in cervical squamous carcinoma (SiHa) cells. Clin Diagn Lab Immunol 2002;9: 1102–1106.
37. Chelbi-alix MK, Bobe P, Benoit G, Canova A, Pine R. Arsenic enhances the activation of Stat1 by interferon gamma leading to synergistic expression of IRF-1. Oncogene 2003;22:9121–9130.
38. Matikainen S, Lehtonen A, Sareneva T, Julkunen I. Regulation of IRF and STAT gene expression by retinoic acid. Leuk Lymphoma 1998;30:63–71.
39. Altucci L, Rossin A, Raffelsberger W, Reitmair A, Chomienne C, Gronemeyer H. Retinoic acid-induced apoptosis in leukemia cells is mediated by paracrine action of tumor-selective death ligand TRAIL. Nat Med 2001;7:680–686.
40. Clarke N, Jimenez-Lara AM, Voltz E, Gronemeyer H. Tumor suppressor IRF-1 mediates retinoid and interferon anticancer signaling to death ligand TRAIL. EMBO J 2004;23:3051–3060.

Received April 21, 2005. Accepted November 30, 2005.

Address requests for reprints to: Benjamin C. Y. Wong, MD, Department of Medicine, University of Hong Kong, Hong Kong, China. e-mail: bcywong@hku.hk; fax: (852) 2872-5828.

Supported by grants from the Research Grant Council of Hong Kong Special Administrative Region (HKU 7482/03M), and the Gastroenterological Research Fund of the University of Hong Kong, Hong Kong.